Functional Paper-based Platform for Rapid Capture and Detection of CeO$_2$ Nanoparticles

Ali Othman,[a] Daniel Andreescu,[a] Dinusha P. Karunaratne,[a] S. V. Babu[b,c], and Silvana Andreescu*[ab]

[a] Department of Chemistry and Biomolecular Science, Clarkson University, Potsdam, New York 13699-5810, USA. E-mail: eandrees@clarkson.edu; Fax: +(315) 268 6610; Tel: +(315) 268 2394

[b] Department of Chemical and Biomolecular Engineering, Clarkson University, Potsdam, New York 13699, USA

[c] Center for Advanced Materials Processing, Clarkson University, Potsdam, New York 13699, USA

Nanoparticle Concentration Calculation (NP/mL). The number of nanoparticles (N_{np}) per mL was estimated based on the particle size distribution analysis, assuming a spherical particle with a volume (V_{np}) of $4/3\pi r^3$ where r is the average radius of the NPs as determined by DLS measurements (17.6 nm). The weight of a single particle (W_{np}) was calculated by considering the density of CeO_2 NPs (D_{np}) to be equivalent to that of the bulk phase (e.g., 7.65 g/mL)[1-2]. For example, the volume of CeO_2 NPs with an average diameter of 17.6 nm is 2.85×10^{-18} mL and the W_{np} is 2.2×10^{-17} g per particle. Using this data and the concentration of CeO_2 NPs in colloidal solution in µg/mL we find the N_{np} of 2.3×10^{11} NP/mL for a solution of 5 ppm. For all types of particles, the NPs/mL concentrations were calculated according with their size.
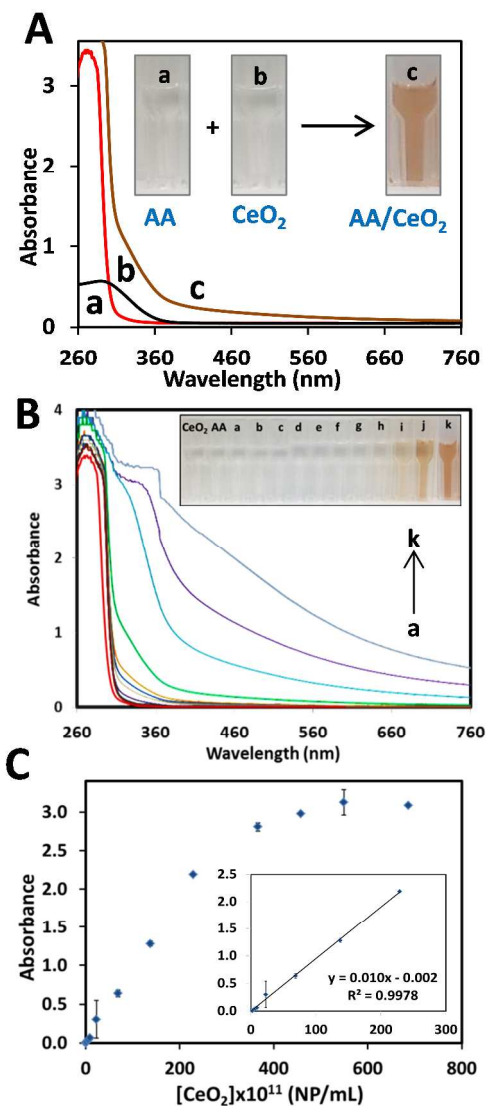
Figure S1. ***(A)*** *Spectroscopic responses and UV-Vis spectra of ascorbic acid (AA), at 5 mM and pH 3.0, in the absence and presence of CeO₂ NPs dispersion.* ***(B) and (C)****. Concentration dependent spectral changes with increasing the NPs concentration (from a to k: (0.46, 0.57, 1.14, 2.28, 4.6, 6.9, 9.2, 22.9, 68.7, 137.4 and 229) x10¹¹ NP/mL)) and the corresponding calibration curve and linear range recorded at λ$_{max}$ = 435 nm. Error bars represent standard deviations for n = 3 measurements.*
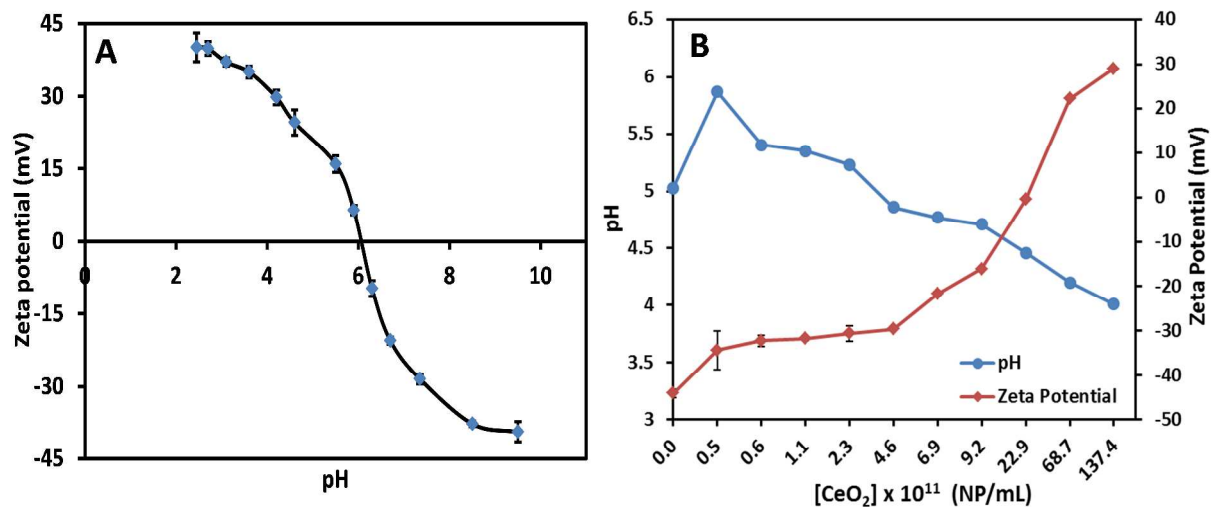
Figure S2. **A)** *Zeta-potential (ξ) of the CeO₂ NPs suspension (1.4x10¹³* NP/mL*) versus pH,* **B)** *Changes in pH and surface charge (ξ) as a function of CeO₂ NPs concentration in the presence of catechol (5 mM, pH 5), (n=5).*
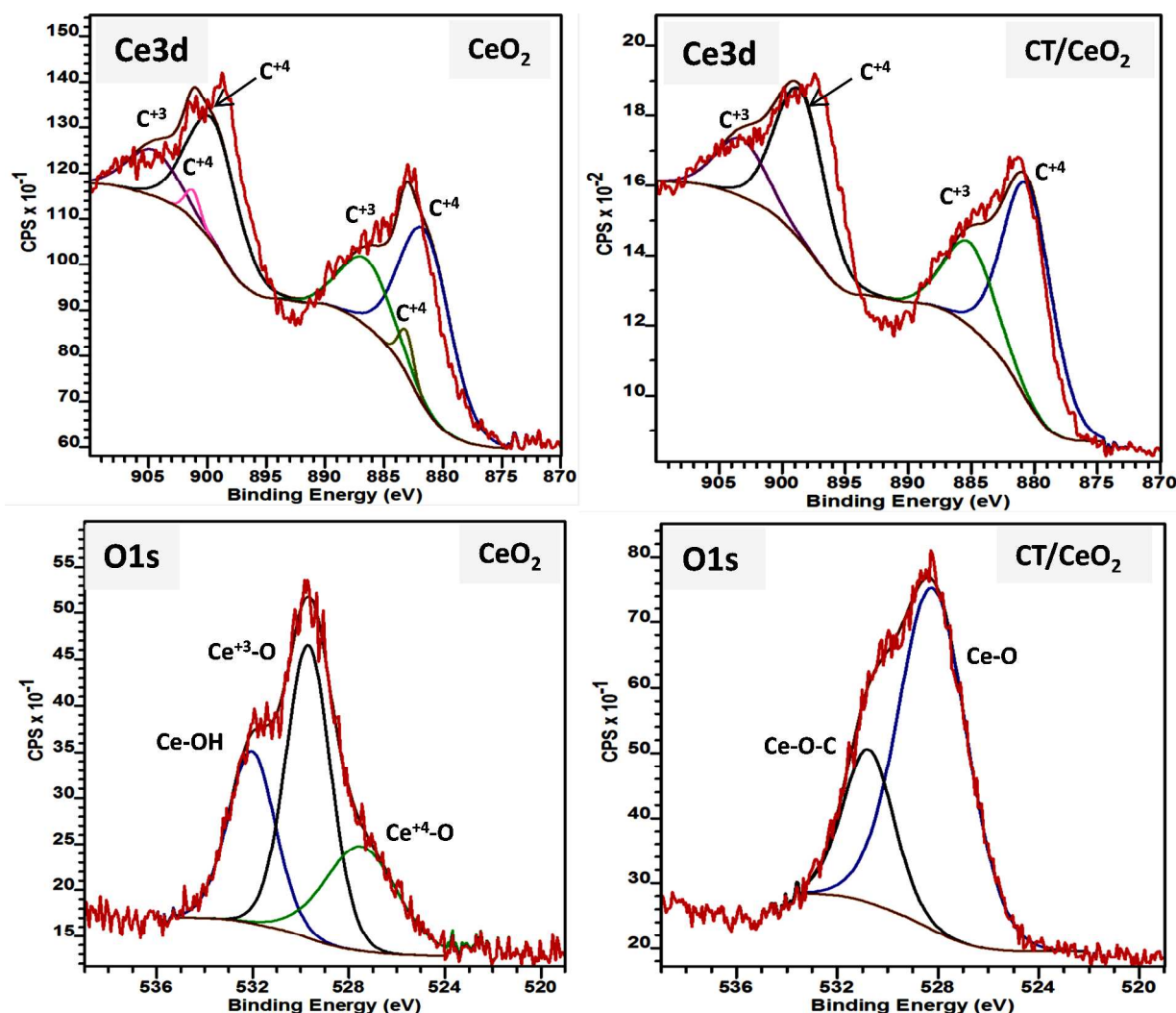
Figure S3.*Ce3d and O1s XPS spectra of CeO₂ NPs and CT/CeO₂ NPs.*

Table S1: *XPS data resulting from the fitting of the Ce 3d spectra of CeO₂ NPs and CT/CeO₂ NPs.*

Sample	CeO₂						CT/CeO₂					
Peak Position (eV)	881.5	883.1	886.6	899.6	901.2	904.6	880.5	880.8	885.1	898.6	898.9	903.4
Peak Area	2107.7	152.4	791.9	1459.6	105.5	548.4	3076	0.0	1198.2	2130.2	0.0	829.8

A

100 μm

B

10 μm

C

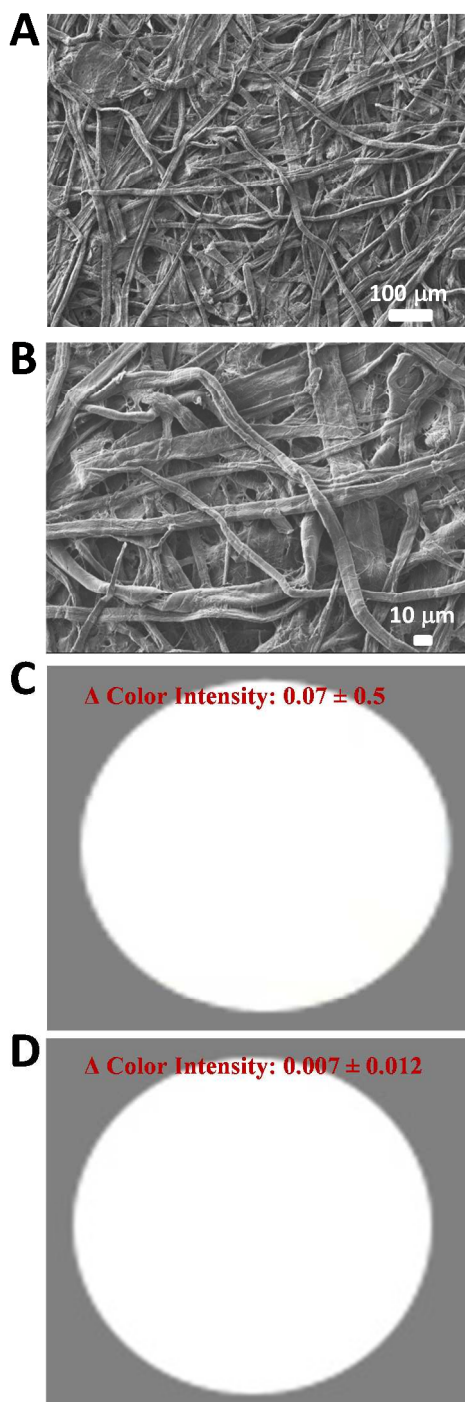Δ Color Intensity: 0.07 ± 0.5

D

Δ Color Intensity: 0.007 ± 0.012

Figure S4. SEM images of the control non-functionalized paper after exposure to CeO_2 NPs $(9.2x10^{13}$ NP/mL) at a magnification of 100 μm (**A**) and 10 μm (**B**). **C**. Color response of the filter paper after exposure to CeO_2 NPs $(9.2x10^{13}$ NP/mL). **D.** Color response of bare paper disc.
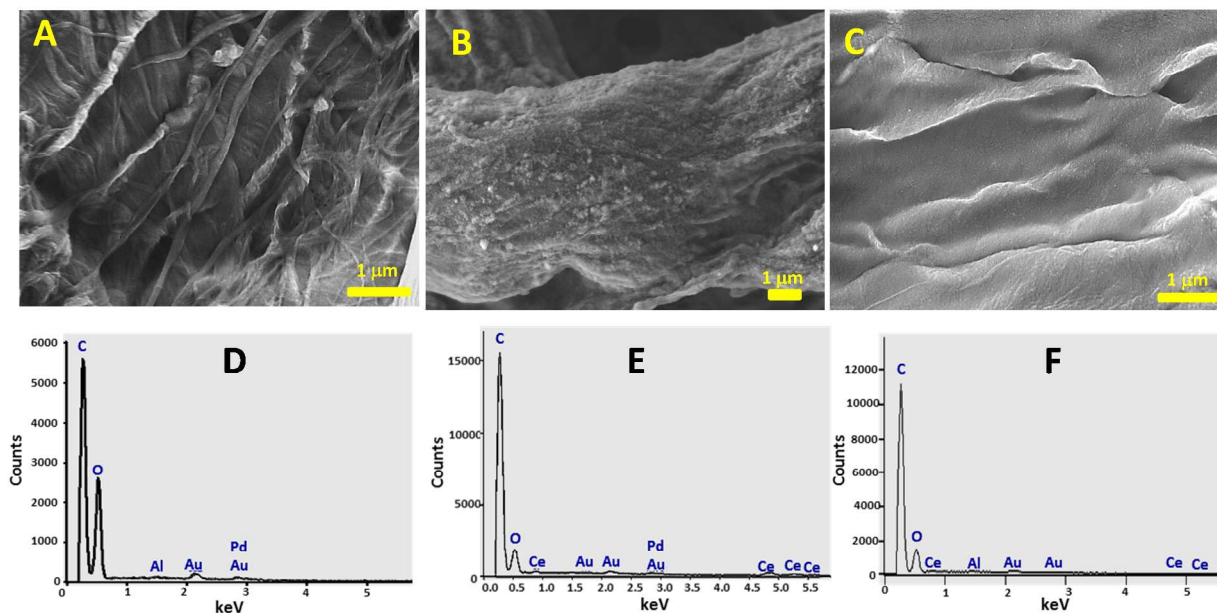
Figure S5. SEM images of the cellulosic paper filter after ligand grafting (*A*) and after exposure to CeO$_2$ NPs (9.2x10^{13} NP/mL) (*B*). SEM image of the paper filter without ligand grafting (catechol) after exposure to CeO$_2$ NP (9.2x10^{13} NP/mL) (*C*). *D*, *E* and *F*: corresponding EDX analysis of A, B, and C samples, respectively.
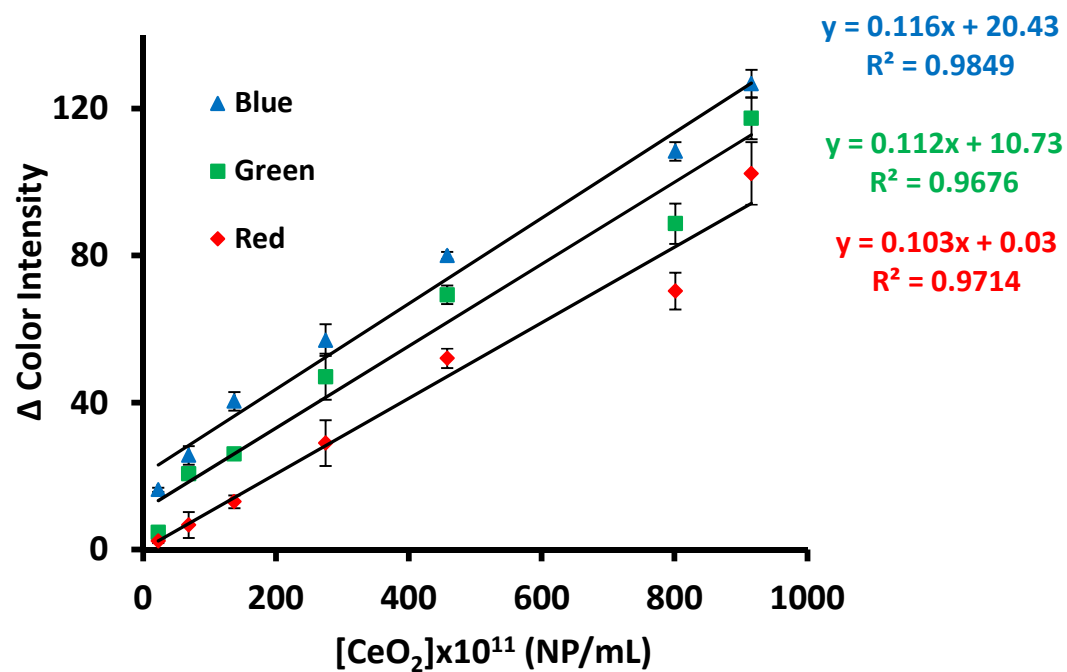
Figure S6: *Quantified color intensity of catechol-grafted paper upon exposure to different concentrations of CeO$_2$ NPs using different RGB color channels (blue, green, and red).*
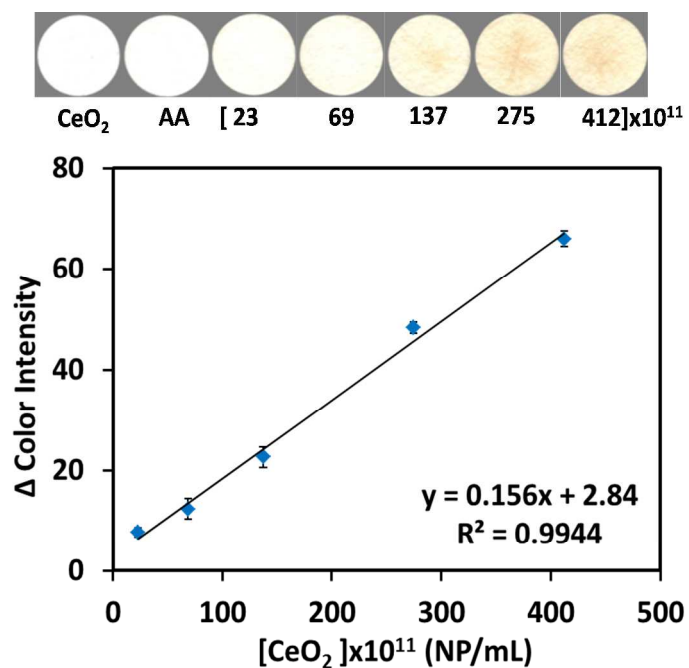
Figure S7. *Colorimetric responses of AA-grafted paper for upon exposure to different concentrations of CeO$_2$ NPs and their corresponding calibration curve of the Δ color intensity (average responses and standard deviation for n = 3).*
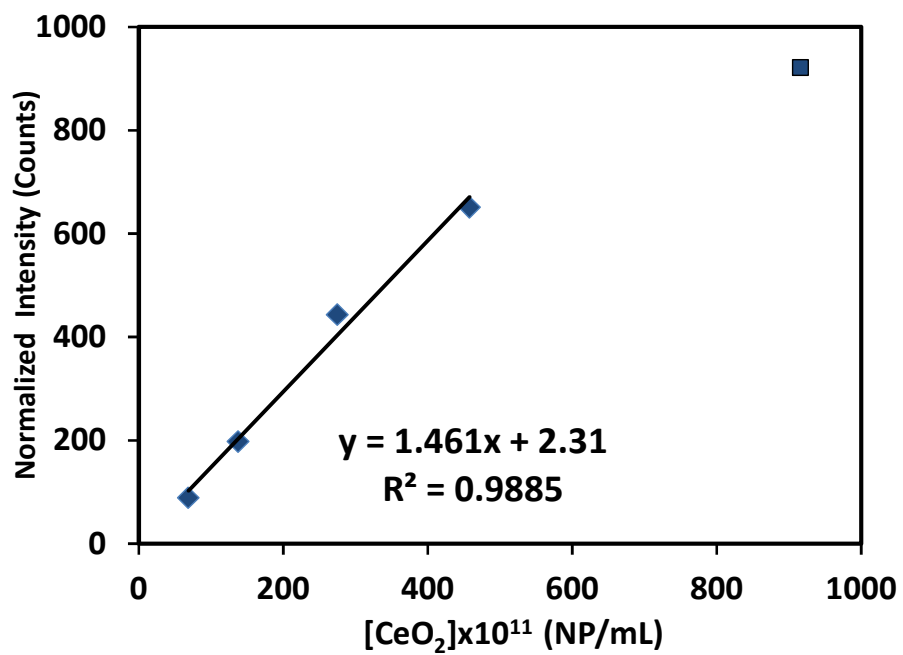
Figure S8. *XRF calibration curve of catechol-grafted cellulosic paper upon exposure to increasing CeO₂ NPs concentrations.*

Table S2: Characteristics of CeO$_2$ NPs with different types of surface coating

Sample	Source	Surface modification	Nature of NPs	NPs Size (nm)
A	Synthesized[a]	Polyacrylic acid-Oleylamine (PAA-OA) copolymer	Colloidal, 10 % dispersion in 0.1 M Na$_2$CO$_3$, high pH	< 10
B	Commercial modified	No information Sigma-Aldrich, #544841	nanopowder, washed and dried at 105 ^{o}C	< 25
C	Synthesized[b]	Citric acid	nanopowder	< 10
D	Synthesized[c]	Glycine	nanopowder	20-40
E	Synthesized	PAA-OA calcined at 300 ^{o}C	nanopowder	< 10

[a] Synthesized following a procedure of synthesis of crystalline ceria *via* thermal decomposition of cerium precursors [1].

[b] Synthesized following a procedure of synthesis of ceria-modified- *via* thermohydrolysis of an acidic solution of cerium-IV nitrate salt Ce(NO3)4 at high temperature.[3]

[c] Synthesized following a procedure of surface modification of ceria nanoparticles.[4]
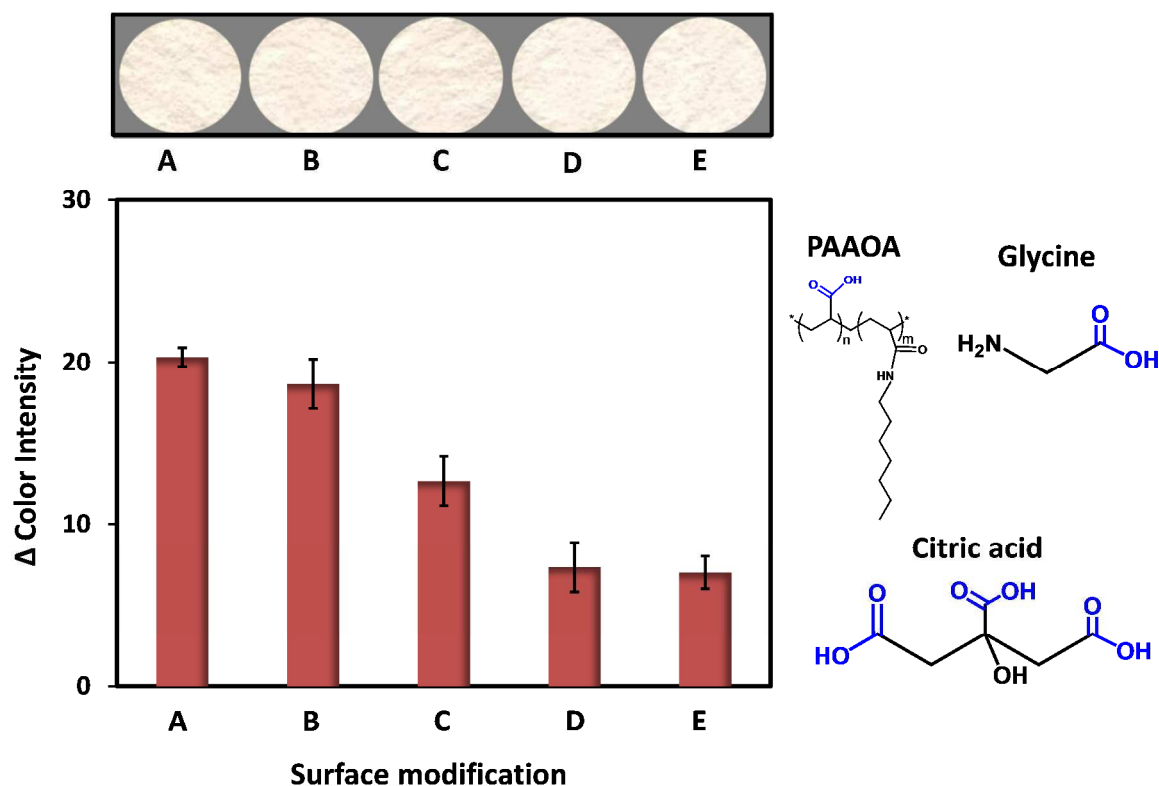

*Figure S9. Colorimetric responses of paper sensors upon addition of CeO$_2$ NPs dispersions (9.2x10^{13} NP/mL) with different coating agents to the catechol functionalized filter; **A)** Polyacrylic acid-Oleylamine (PAA-OA), **B)** CeO$_2$ NPs <25 nm (nanopowder), washed and dried at 105 ^{o}C, **C)** Citric acid, **D)** Glycine, **E)** Polyacrylic acid-Oleylamine (PAA-OA) modified.*

(A)

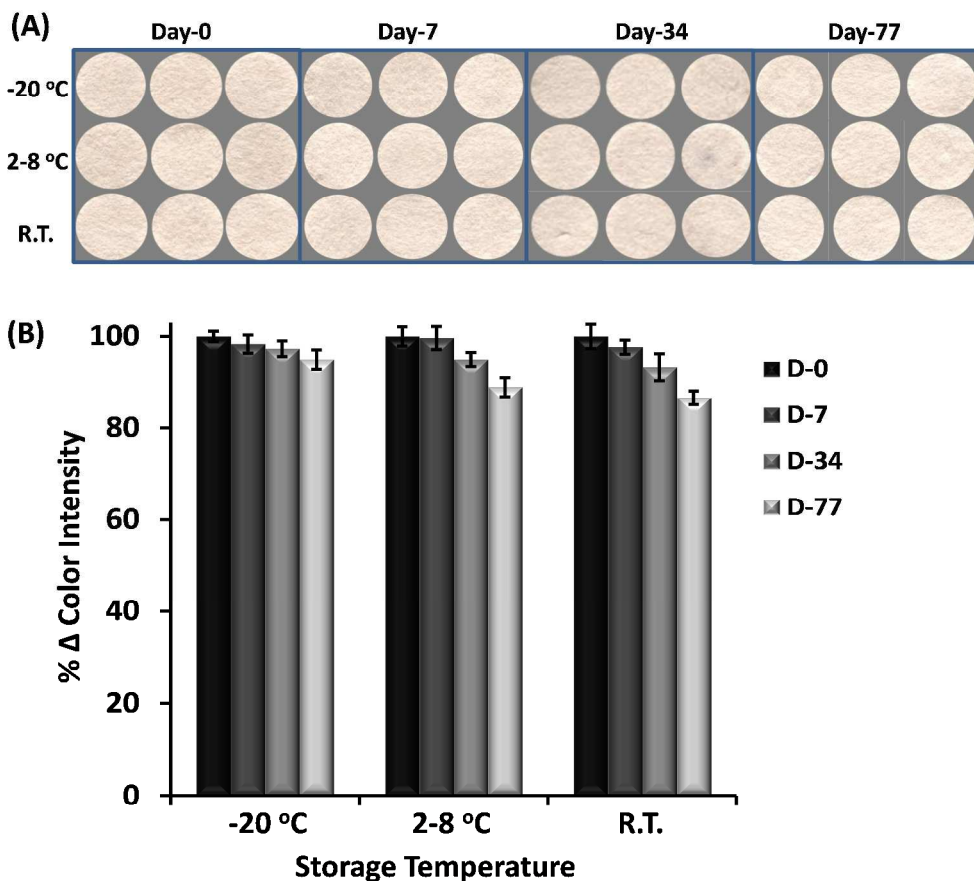|	Day-0	Day-7	Day-34	Day-77
-20 ºC				
2-8 ºC				
R.T.				

(B)

Figure S10. A) Storage stability of the catechol-functionalized filters quantified by the color change upon exposure to NPs upon storage in three different conditions: room temperature (~25 ºC), refrigerator (2-8 ºC) and freezer (~ -20 ºC). Responses are quantified as the color intensity of the paper disks after addition of CeO$_2$ NPs (68.7x10^{11} NP/mL), (n = 3). B) Histograms showing % decrease of response (with day 0 corresponding to 100%).
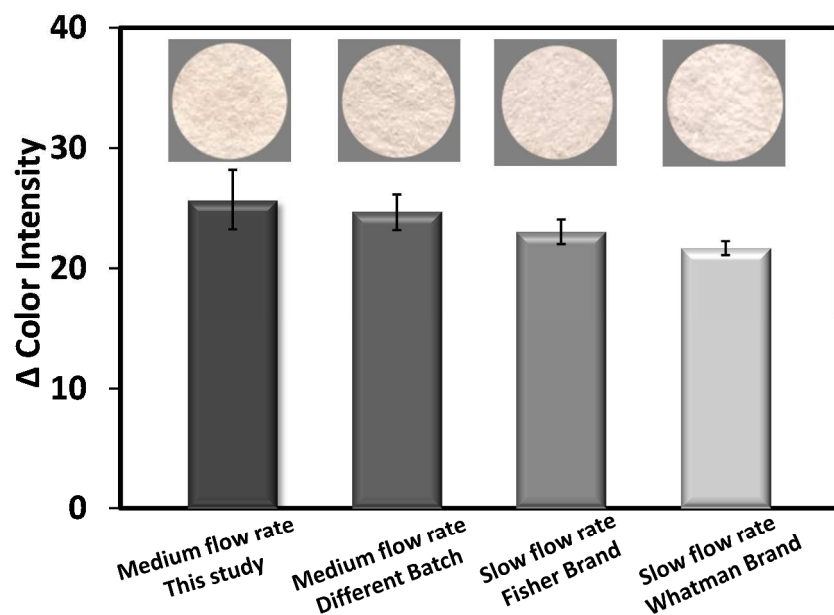
Figure S11. *Colorimetric response of different types of cellulosic filter papers functionalized with catechol upon exposure to the same concentration of CeO₂ NPs (68.7x10¹¹ NP/mL). From left to right: filter papers with medium flow rate used in this study (the first two columns show paper from different batches), and filter papers with slow flow rate from Fisher Scientific and Whatman brands, respectively,(n=3).*

Table S3: Characteristics of different types of metal oxides tested in the selectivity study.

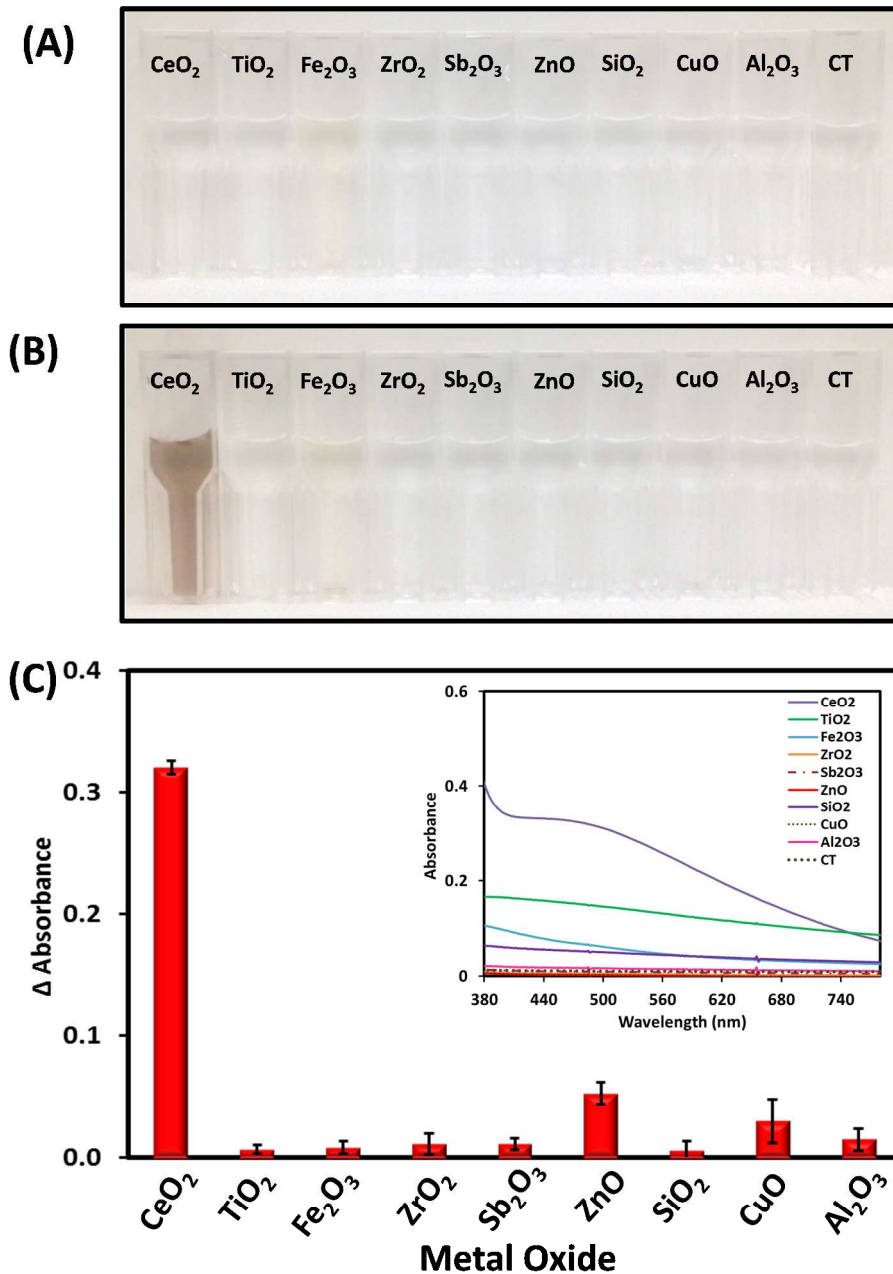| Particles	Nature of NPs	NPs Size (nm)
TiO_2	nanopowder	10-30
Fe_2O_3	nanopowder	20-40
ZrO_2	nanopowder	40
Sb_2O_3	nanopowder	80-200
ZnO	nanopowder	10-30
SiO_2	Colloidal, 30 % SiO_2, acidic	35
CuO	nanopowder	40
Al_2O_3	nanopowder	300

Figure S12. *Colorimetric responses **A)** before and **B)** after addition of different types of metal oxide NP dispersions (68.7x10^{11} NP/mL) to catechol solution (5 mM), and **C)** Comparative absorbance changes and corresponding UV-Vis spectra of catechol-metal oxide conjugates for the same NP concentration.*

Table S4: Color codes of catechol-grafted filter papers upon exposure to different types of metal oxides. The color codes were obtained from Adobe Photoshop software.

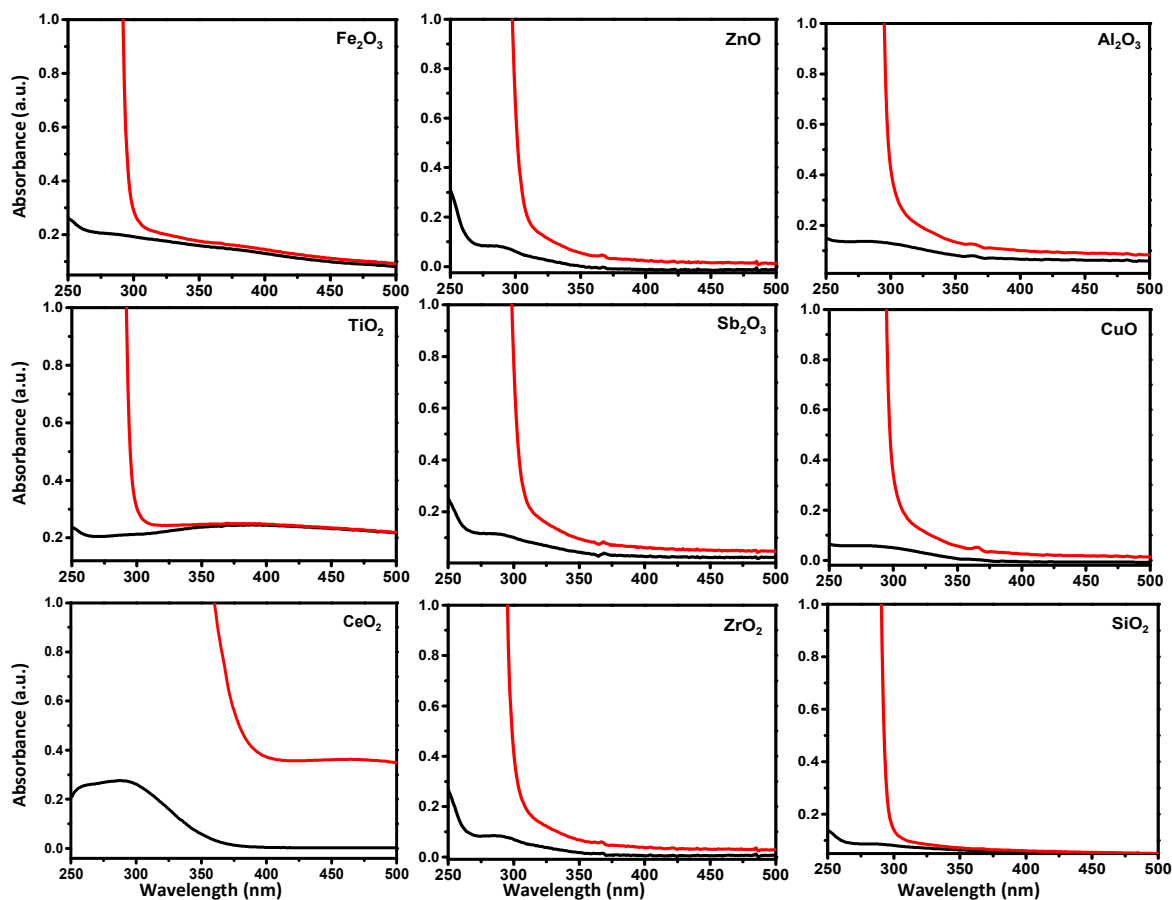| Metal Oxide	Color Code No.
CeO_2	F1DED5
TiO_2	FFFDF6
Fe_2O_3	F6F1EB
ZrO_2	FBFBF3
Sb_2O_3	FEFFFA
ZnO	FCFBF5
SiO_2	F9F9EE
CuO	FAF6ED
Al_2O_3	FDFDF1

Figure S13. *UV-Vis spectra of the varying metal oxide NPs at the same concentration tested in this work before (black) and after (red) reaction with catechol solution (5 mM, pH 5).*
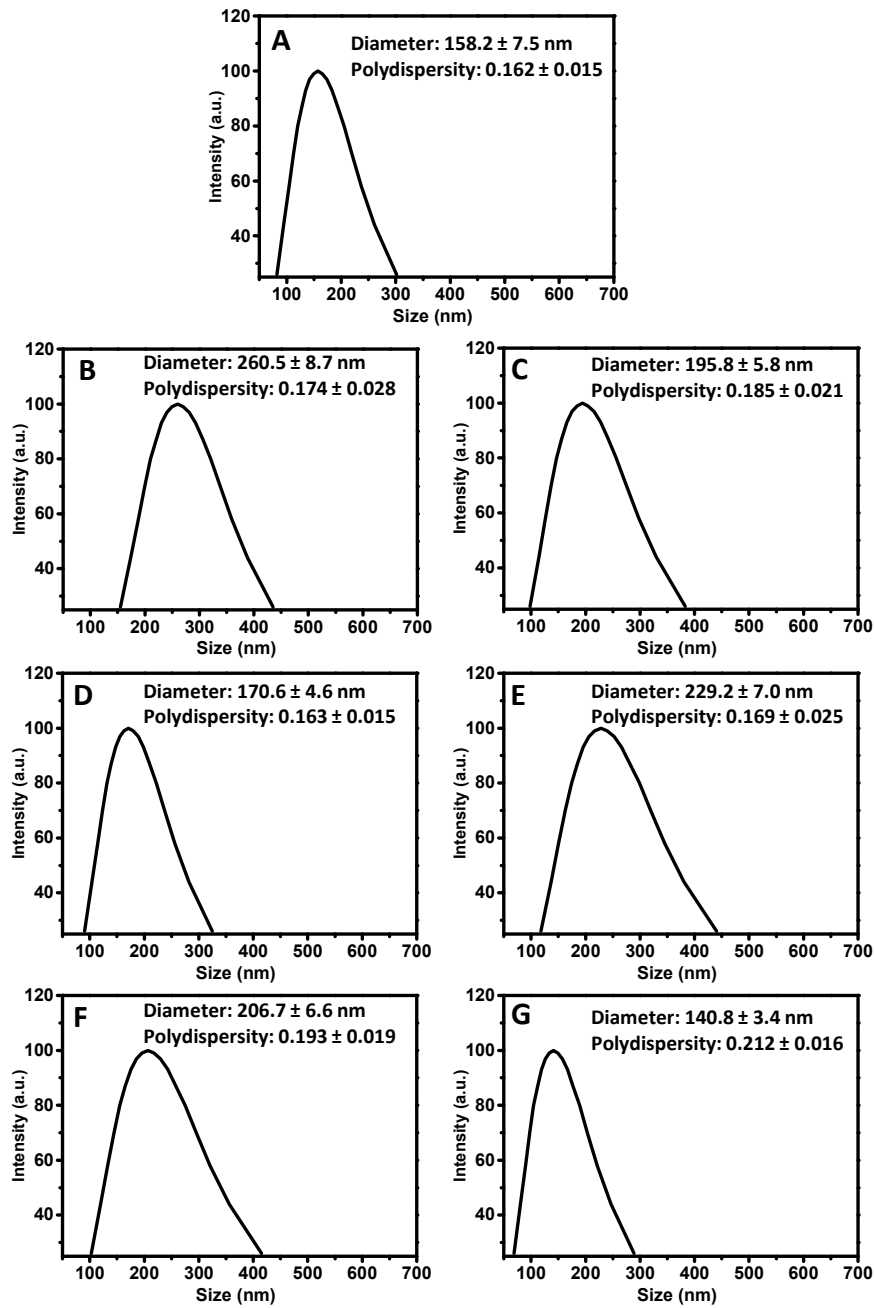
Figure S14. *Size distribution data of **(A)** the abrasive CeO₂ used for CMP polishing process (140 nm, supplied by Ferro Corp. (50 wt. %)). And data of waste samples collected from CMP polishing, from **(B)** to **(G)**: CGS/SiN, CGS/SiO₂, CPS/SiN, CPS/SiO₂, C/SiO₂: 3.125 wt %, and C/SiO₂: 6.25 wt %, respectively.*

Table S5. Comparison of measurement performance of the proposed platforms *versus* other NP-colorimetric detection methods reported in the literature.
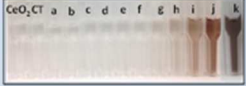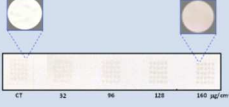
Ref.	LOD	LOQ	Response / Real sample	Linear ranges	Detection principle
This work	0.36×10^{11} NP/mL	1.2×10^{11} NP/mL	Visual detection within seconds. Responds for CeO_2 as well to other oxides NPs such as TiO_2, Fe_2O_3, Sb_2O_3, ZnO, ZrO_2, CuO, SiO_2, and Al_2O_3	CeO_2 NPs ranging from $(0.46 – 5.5) \times 10^{11}$ NP/mL	Ability of CeO_2 NPs to react selectively via oxidative and surface chelation processes with readily oxidizible ligands containing o-dihydroxy functionalities, such as catechol and ascorbic acid.
This work	14.9×10^{11} NP/mL	49.7×10^{11} NP/mL	Responds for CeO_2 as well to other oxides NPs such as TiO_2, Fe_2O_3, Sb_2O_3, ZnO, ZrO_2, CuO, SiO_2, and Al_2O_3 CMP wastewater	CeO_2 NPs ranging from $23 \times 10^{11} – 9.2 \times 10^{13}$ NP/mL	Surface confined colorimetric response of ligand-functionalized platform exposed to NPs
This work	4.5×10^{11} NP/mL	15×10^{11} NP/mL	Responds for CeO_2 NPs	CeO_2 NPs ranging from $(23 – 115) \times 10^{11}$ NP/mL	Microarray detection spots created by nanodot printing
Ref[5]	89-1,759 µg/L	526-5,864 µg/L	Responds to both metals (e.g., Ag and Au) and oxide NPs Environmental water (e.g., lake water, NOM) and biological matrices (e.g., artificial urine, mouse serum).	Wide range of metals (e.g., Ag and Au) and oxide (e.g., CeO_2, SiO_2, VO_2) NPs with a diameter range of 5 to 400 nm and multiple capping agents.	Solution-based colorimetric method for generalNP measurements
Ref[6]	100-1000 µg/L	---	Measurements of various sizes and shapes of Au nanostructures No real sample demonstrated	Detection varies with various types of NPs	Using changes in the visible absorbance spectra of dyes in aqueous solutions before and after exposure to the NPs
Ref[7]	2.0 µg/mL	---	Measurements of types of MnO_2 nanosheets Real lake water	Solution-based naked eye detection	Detection soluble TMB dye

Table S6: Comparison of the performance characteristics of the different techniques for detection of CeO_2 NPs used in the study.

Technique/Characteristics	Linear Range (NP/mL)	LOD (NP/mL)	LOQ (NP/mL)
Spectroscopic	$(0.46 – 5.5) \times 10^{11}$	0.36×10^{11}	1.2×10^{11}
Paper sensor	$23 \times 10^{11} – 9.2 \times 10^{13}$	14.9×10^{11}	49.7×10^{11}
XRF of paper sensor	$68.7 \times 10^{11} – 4.6 \times 10^{13}$	4.7×10^{11}	15.7×10^{11}
Microarray printing	$(23 – 115) \times 10^{11}$	4.5×10^{11}	15×10^{11}

REFERENCES

1.   Lee, S. S.; Zhu, H.; Contreras, E. Q.; Prakash, A.; Puppala, H. L.; Colvin, V. L., High Temperature Decomposition of Cerium Precursors to Form Ceria Nanocrystal Libraries for Biological Applications. *Chem. Mater.* **2012,** *24* (3), 424-432.
2.   Tom, R. T.; Suryanarayanan, V.; Reddy, P. G.; Baskaran, S.; Pradeep, T., Ciprofloxacin-Protected Gold Nanoparticles. *Langmuir* **2004,** *20* (5), 1909-1914.
3.   Sehgal, A.; Lalatonne, Y.; Berret, J.-F.; Morvan, M., Precipitation-Redispersion of Cerium Oxide Nanoparticles with Poly (Acrylic Acid): Toward Stable Dispersions. *Langmuir* **2005,** *21* (20), 9359-9364.
4.   Zhang, Z.; Yu, L.; Liu, W.; Song, Z., Surface Modification of Ceria Nanoparticles and Their Chemical Mechanical Polishing Behavior on Glass Substrate. *Appl. Surf. Sci.* **2010,** *256* (12), 3856-3861.
5.   Corredor, C.; Borysiak, M. D.; Wolfer, J.; Westerhoff, P.; Posner, J. D., Colorimetric Detection of Catalytic Reactivity of Nanoparticles in Complex Matrices. *Environ Sci Technol* **2015,** *49* (6), 3611-3618.
6.   Mahmoudi, M.; Lohse, S. E.; Murphy, C. J.; Suslick, K. S., Identification of Nanoparticles with a Colorimetric Sensor Array. *ACS Sensors* **2015,** *1* (1), 17-21.
7.   He, Y.; Wang, Z.; Long, D., Direct Visual Detection of Mno2 Nanosheets within Seconds. *Analytical and Bioanalytical Chemistry* **2016,** *408* (4), 1231-1236.